Dewetting of thin films on heterogeneous substrates: Pinning versus coarsening

Lutz Brusch,[1] Heiko Kühne,[1] Uwe Thiele,[1,2,*] and Markus Bär[1,†]
[1]*Max-Planck-Institut für Physik komplexer Systeme, Nöthnitzer Straße 38, D-01187 Dresden, Germany*
[2]*Department of Physics, University of California, Berkeley, California 94720-7300*
(Received 14 November 2001; revised manuscript received 2 May 2002; published 19 July 2002)

We study a model for a thin liquid film dewetting from a periodic heterogeneous substrate (template). The amplitude and periodicity of a striped template heterogeneity necessary to obtain a stable periodic stripe pattern, i.e., pinning, are computed. This requires a stabilization of the longitudinal and transversal modes driving the typical coarsening dynamics during dewetting of a thin film on a homogeneous substrate. If the heterogeneity has a larger spatial period than that of the critical dewetting mode, weak heterogeneities are sufficient for pinning. Our results imply a large region of coexistence between coarsening dynamics and pinning.

DOI: 10.1103/PhysRevE.66.011602 PACS number(s): 68.15.+e, 47.20.Ky, 47.20.Ma, 68.55.−a

Templating and controlled rupture of liquid films on chemically structured substrates have provoked many experimental efforts [1–6] but the conditions for the desired imaging of the template structure onto the deposit pose many open questions. First theoretical results for liquid layers on structured surfaces with strong heterogeneities of wettability, i.e., stepwise alternating hydrophilic and hydrophobic stripes in an aqueous system, describe different morphological transitions when changing the size of the heterogeneous patches or the volume of the deposited liquid [7–10]. Experimentally, the challenge of preventing the dewetting pattern from coarsening has been met by evaporation of the solvent [11], by literally freezing the system [12], or by using a heterogeneous substrate [1].

In the present paper we study the transition between coarsening and pinning for thin films on weakly structured substrates that possess spatial modulations of the molecular interaction terms. There is no well-defined contact line for the scales under investigation and consequently, we do not consider the pinning of a contact line to defects of the substrate surface. Here we use the term ''pinning'' if the liquid ridges of the asymptotic film profile match the more wettable stripes of the substrate. Thin films on homogeneous substrates can be unstable to spinodal dewetting, see e.g., [13,14]. Sharma and coworkers proposed a model that contains polar and apolar components of molecular interactions and reproduced the dynamics of dewetting thin films [15]. Recently, it has been shown that this model has periodic stripe solutions that are unstable to coarsening [16]. Here, we use a slightly different model derived from diffuse interface theory by Pismen and Pomeau [17]. We emphasize that this model has very similar dynamics [18] and stationary solutions [19] as the Sharma model. The impact of a heterogeneous substrate on the stationary film profiles, their linear stability, and resulting conditions for morphological transitions are presented. The dynamics of thin films on periodic stripe templates have been studied in Ref. [10] with the original Sharma model by numerical integration and for a given heterogeneity of large amplitude. Using bifurcation and stability analysis, we can provide, however, a more systematic study of the effects of parameters such as average film thickness $\bar{h}$, amplitude ϵ, and spatial period P_{het} of the heterogeneity.

Our starting point is a homogeneous or weakly heterogeneous substrate. We choose parameters in the unstable regime [cross in Fig. 1(a)]. Then a striped solution of a spatial period $P=P_{het}$ is considered. For illustration we display a system of length $2P_{het}$ [see Figs. 1(b)–1(e)]. The periodic stripe pattern [Fig. 1(b)] is now unstable against several transversal [Fig. 1(c)] and longitudinal [Figs. 1(d) and 1(e)] perturbations. Stability analysis allows us to trace the corresponding eigenvalues. Increasing the strength of the heterogeneity, they all will acquire negative real parts and the desired pattern in Fig. 1(b) is pinned, i.e., becomes stable against small perturbations.

The evolution equation for the film thickness profile $h(x,y,t)$ contains a disjoining pressure that is derived by combining the Stokes equation in long wave approximation [20] with diffuse interface theory [17],

$$\partial_t h = -\nabla\{(h-\ln a)^3 \nabla[\Delta h - \partial_h f(h,x)]\}, \qquad (1)$$

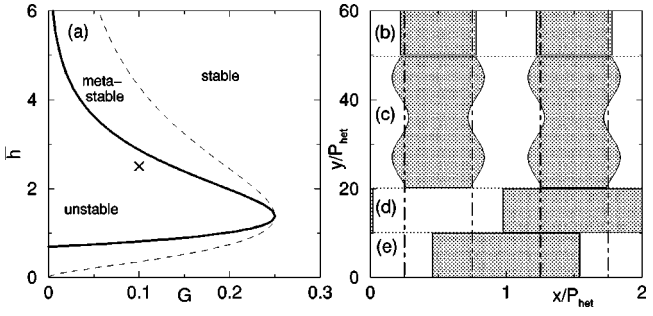

FIG. 1. (a) Phase diagram for thin films on a homogeneous substrate (after Ref. [19]). The cross shows the parameter values for which we present results in detail. (b) Schematic display of the template (dot-dashed line), the periodic film profile with the same spatial period (solid line). Shaded areas show where $h>\bar{h}$. (c) Initial stage of the transversal instability and (d),(e) final stages of variants of the longitudinal coarsening instability.

*Electronic address: thiele@mpipks-dresden.mpg.de
†Electronic address: baer@mpipks-dresden.mpg.de

with a free energy $f(h,x)=\kappa(x)e^{-h}(e^{-h}-2)+\frac{1}{2}Gh^2$ and the ratio G of gravitation to mean molecular interactions as well as the spatially varying strength of the molecular interactions $\kappa(x)$. $a>0$ is a small parameter describing the wetting properties in the regime of partial wetting [17,19]. This dimensionless form is obtained after scaling the original quantities as in Ref. [19]. The molecular interactions that become important on the nanometer scale [21] are incorporated through the disjoining pressure $\Pi(h)$ contained in the derivative of the free energy $\partial_h f(h,x)=-\kappa(x)\Pi(h)+Gh$. The chosen $\Pi(h)$ is qualitatively equivalent to other pressures consisting of destabilizing short range and stabilizing long-range interactions [20] but does not suffer from the usual divergency for vanishing film thickness [19]. In the absence of heterogeneity, the model possesses two control parameters, the ratio G and the average film thickness $\bar{h}$ that is chosen as a conserved quantity. A phase diagram in G and $\bar{h}$ indicating the region of spinodal dewetting is shown in Fig. 1(a).

Heterogeneous substrates with a smooth change in the wettability are modeled by a spatial sinusoidal modulation of the overall strength of the disjoining pressure,

$$\kappa(x)=1+\epsilon\cos(2\pi x/P_{het}). \tag{2}$$

The system behavior is controlled by the amplitude ϵ and the imposed periodicity P_{het} of the heterogeneity. Droplets are preferably located at minima of $\kappa(x)$. Our choice of $\kappa(x)$ introduces a single length scale P_{het} and serves as a starting point for analyzing more realistic choices with several scales.

We choose the system size, L multiple of P_{het}, use periodic boundary conditions and vary $\epsilon\geqslant 0$. The energy of a striped solution $h(x,t)$ is given by the Lyapunov functional [19]

$$E=\frac{1}{L}\int_0^L\left[\frac{1}{2}(\partial_x h)^2+f(h,x)\right]dx. \tag{3}$$

During the time evolution of a given initial film thickness profile this energy decreases and eventually settles in a minimum when the system approaches a linearly stable stationary solution of Eq. (1). One can determine these solutions directly by setting $\partial_t h=0$ in Eq. (1) and integrating twice [19], yielding

$$0=\partial_{xx}h-\partial_h f(h,x)+C_1. \tag{4}$$

The integration constant C_1 and the spatial period P now parametrize a two-parameter family of periodic solutions, i.e., periodic patterns of holes and droplets, that can be calculated by continuation techniques [23]. P can be equal to P_{het} or its multiples. Focusing on situations with conserved liquid volume we adopt the mean film thickness $\bar{h}=1/L\int_0^L h(x)dx$ as the second parameter beside the period, using C_1 as a Lagrange multiplier. Typical film profiles are shown in Figs. 2(a) and 2(b).

For homogeneous substrates with $\epsilon=0$, flat films are stationary solutions that, depending on mean film thickness and the parameter G, may be unstable to infinitely small (spinodal dewetting) or finite (nucleation) disturbances of the film surface. Rupture due to the spinodal mechanism occurs for perturbations with periods larger than a critical value, $P_c=2\pi/k_c$ with $k_c^2=-\partial_{hh}f(h,x)|_{\bar{h}}$ [19]. On a slower time scale the initially formed holes coalesce, the pattern becomes coarser and tends to the absolute minimum of the energy at the largest possible P, i.e., the system size.

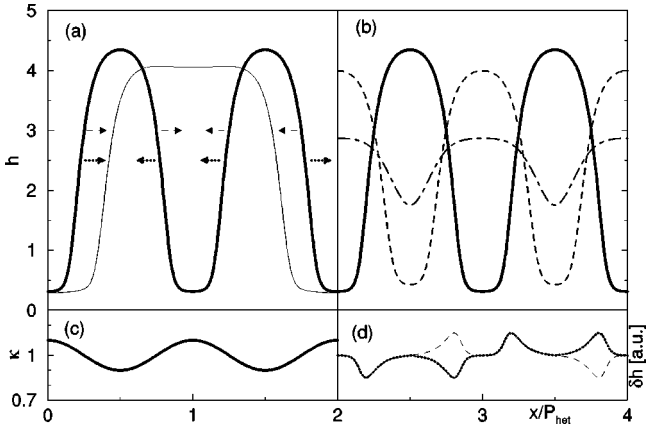

FIG. 2. (a) Stationary film profiles to Eq. (1) with $P=P_{het}$ (thick line) and $P=2P_{het}$ (thin line). (b) Portraits of all solutions with $P=P_{het}$. Only the solid profile is linearly stable. (c) The heterogeneity and (d) the two coarsening modes due to translation (dashed line) and transfer of mass (dotted line) as sketched in (a). Parameters are $\epsilon=0.1$, $G=0.1$, $\bar{h}=2.5$, and $P_{het}=50$.

(i) *Perturbation theory*. If the heterogeneity is switched on, the flat film is no longer a solution to Eq. (4). However, for very small $\epsilon\ll 1$ an analytical expression for the weakly varying stationary film profile can be calculated. Rewriting the heterogeneity as $\epsilon(e^{ik_{het}x}+\text{c.c.})/2$ with $k_{het}=2\pi/P_{het}$ and using the volume conserving ansatz $h(x)=\bar{h}+\alpha(e^{ik_{het}x}+\text{c.c.})/2$ with $O(\alpha)=O(\epsilon)$ in Eq. (4), gives to first order in ϵ a stationary solution with $\alpha=-\epsilon\Pi(\bar{h})/(k_c^2-k_{het}^2)$. This solution is only valid for $\alpha\ll 1$. For $P_c<P_{het}$, the solution is modulated in phase with the heterogeneity, whereas for $P_c>P_{het}$ the phase is shifted by π. Results obtained by perturbation theory are depicted in Fig. 3(b).

(ii) *Numerical bifurcation results*. Suppose a variety of heterogeneous substrates with appropriate period P_{het} but different ϵ is available and a dewetting pattern with spatial period $P=P_{het}$ is desired. We choose a linearly unstable mean film thickness $\bar{h}$ such that the critical wavelength of spinodal dewetting P_c is of the same order as P_{het}. As an example, we choose $P_c\approx P_{het}/1.5$ with $P_{het}=50$ and $G=0.1,\bar{h}=2.5$. This ratio of P_{het}/P_c is known to give good templating for strong heterogeneities [10]. The stationary solutions with $P=P_{het}$ and $P=2P_{het}$ are computed [22] as ϵ is increased using the weakly modulated solutions as a starting point for the continuation [23]. Figs. 2(a), 2(b), and 3(a) show profiles of the solutions and the bifurcation diagram and Fig. 3(b) compares the results with perturbation theory. The weakly modulated solutions are indeed in line with the results of perturbation theory. Breaking the translational symmetry at $\epsilon=0$ gives rise to two branches of solutions starting at the large amplitude solution known from the ho-

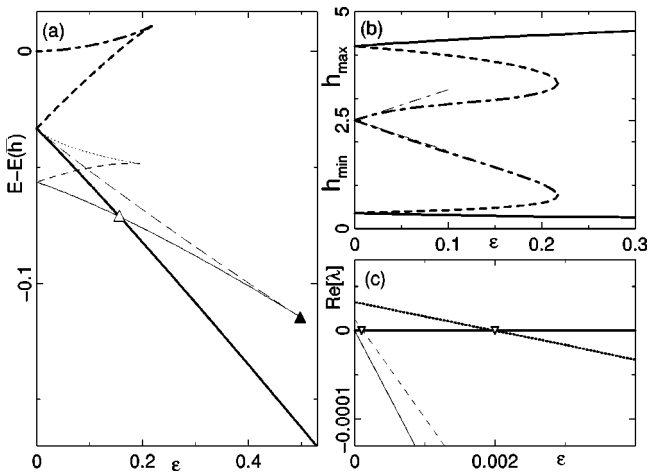

FIG. 3. (a) Relative energy of stationary solutions to Eq. (1) with $P=P_{het}$ (thick line) and $P=2P_{het}$ (thin line) versus ϵ. A flat film at $\epsilon=0$ yields $E(\bar{h})\approx 0.155$. Solid curves correspond to coexisting linearly stable solutions. (b) Bifurcation diagram representing maximum (upper half) and minimum (lower half) of solutions with $P=P_{het}$. Thin dot-dashed lines denote results from perturbation theory and other line styles match with (a) and Fig. 2(b). (c) Eigenvalues λ with largest real part of the lowest energy solutions with $P=P_{het}$ [thick solid branch in (a)]. Solid curves correspond to Goldstone modes at $\epsilon=0$ and broken curves to interaction modes with period $2P$. Line styles match the profiles in Fig. 2(d). Triangles correspond to period doubling bifurcations where solutions with $P=2P_{het}$ emerge. Parameters are $a=0.1$, $G=0.1$, $\bar{h}=2.5$, and $P_{het}=50$ that yields $\alpha/\epsilon\approx 0.7$.

mogeneous case [19]. Only the branch of largest amplitude possesses a phase shift. The branches of solutions in phase cease to exist in a saddle-node bifurcation at $\epsilon\approx 0.22$.

(iii) *Energy and longitudinal stability*. Thick curves in Fig. 3(a) compare the energies [calculated with Eq. (3)] of the different solution branches given in Fig. 3(b). For the chosen parameter values the solutions in phase have always a larger energy than the ones out of phase. When increasing ϵ the energy of the lower branch decreases further indicating that the heterogeneity favors this pattern with $P=P_{het}$. Thin curves in Fig. 3(a) denote solutions with $P=2P_{het}$. To gain more insight into the conditions of pinning the pattern by a heterogeneity, we analyze the linear stability of the stationary solutions in systems of different sizes [24]. For the stability analysis of periodic solutions, one usually employs a Floquet ansatz. This enables us to get the stability of periodic solutions in large systems corresponding to large ratios $n=L/P_{het}$. We find, however, that the most dangerous, potentially unstable longitudinal modes that induce coarsening of dewetting films are already present in systems for $n=2$. Hence, we constrain the discussion to system sizes $L\leqslant 2P_{het}$ in x direction. In the transversal y direction, we had to use much larger length $\approx 30P_{het}$ for a stability analysis, see below.

In the shortest system, i.e., $L=P_{het}$, the entire lower branch in Fig. 3(a) is linearly stable, whereas the two other branches are unstable. For $\epsilon=0$ the linearly stable solution possesses two zero eigenvalues (Goldstone modes) corresponding to translation symmetry and mass conservation. For $\epsilon\neq 0$ the translation symmetry is broken and the corresponding eigenvalue becomes negative [thin solid line in Fig. 3(c)]. Mass conservation is maintained and the corresponding eigenvalue remains zero for all ϵ [thick solid line in Fig. 3(c)].

In a larger system with $L=2P_{het}$, the first stage of coarsening can be studied that is the fastest since nearest neighbors interact and the energy gain is largest. If templating shall be successful then this first stage needs to be prevented by pinning. In the stability analysis of the two periods, two new eigenvalues appear that correspond to asymmetric combinations of the Goldstone modes [see Fig. 2(d)]. They represent two possible modes of coarsening.

(a) Shift of droplets towards each other caused by a combination of opposite translational modes [dashed arrows in Fig. 2(a) and dashed curves in Figs. 2(d) and 3(c)].

(b) Mass transfer between neighboring unmoved droplets caused by a combination of opposite volume modes [dotted arrows in Fig. 2(a) and dotted curves in Figs. 2(d) and 3(c)].

These modes have first been recognized in the Cahn-Hilliard equation [26]. For small ϵ both eigenvalues are positive, implying the instability of the wanted pattern to coarsening. The mass transfer proceeds faster than the shift of droplets. But, as ϵ increases, both become negative, rendering the solution with period P_{het} linearly stable. At the two crossing points period doubling bifurcations occur where stationary solutions of period $P=2P_{het}$ emerge [compare thin branches in Fig. 3(a)]. Altogether, the desired pinning solution with $P=P_{het}$ is linearly stable for $\epsilon>0.002$.

The value of this critical ϵ depends on parameters and the specific form of $\Pi(h)$. Since the two symmetries connected with the coarsening modes are present for arbitrary choices of $\Pi(h)$ the qualitative behavior does not depend on this choice. Accordingly, two pairs of solutions with $P=2P_{het}$ appear in any given system at finite ϵ.

These four branches of solutions with $P=2P_{het}$ [thin curves in Fig. 3(a)] have the following linear stability. Solutions on the dotted branch carry two positive eigenvalues. The short-dashed branch has still one positive eigenvalue that leads to a shift of the pattern towards solutions of the solid branch. The long-dashed branch has one positive eigenvalue and is a saddle that divides evolutions by translation of two droplets towards one on the solid branch or back to the $P=P_{het}$ branch. The entire thin solid branch is linearly stable in $L=2P_{het}$ and represents the coarse solution competing with the desired pattern [see Figs. 1(e) and 2(a)]. Here, at large $\bar{h}$, the coarse profile of lowest energy emerges from the translation mode, whereas for smaller mean film thicknesses ($\bar{h}\leqslant 2$ for $G=0.1$) the coarse profile corresponding to the transfer mode is stable [see Fig. 1(d)] and has lowest energy [25].

(iv) *Coarsening versus pinning*. As seen in (iii), coarsening is favored for $\epsilon<0.002$ and solutions with $P=2P_{het}$ are the only stable ones. Consequently, they also have the lowest energy (for $L=2P_{het}$). For $\epsilon>0.002$, multistability between linearly stable solutions with $P=P_{het}$ and $P=2P_{het}$ occurs and the initial condition selects the final dewetting structure.

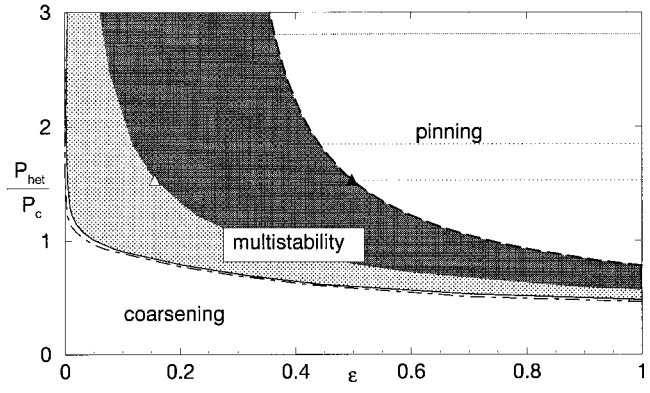

FIG. 4. Morphological phase diagram of templating showing regions in the parameter plane (ϵ, P_{het}) with different behavior of the thin film on a heterogeneous substrate. The shaded band separates parameters of pure coarsening from pure pinning [22]. Inside the shaded band multistability is found with the desired pattern being the energetic minimum inside the dark shaded area. Parameters are $a=0.1, G=0.1, \bar{h}=2.5$, and $P_c \approx 33$. The triangles correspond to the equivalent symbols in Fig. 3(a).

Below $\epsilon \approx 0.157$ the coarse solution has lowest energy, whereas at larger ϵ the desired pinned pattern is energetically favored. Choosing suitable initial conditions enables pinning at much smaller ϵ. But coarsening will still occur at larger ϵ if initial conditions are chosen accordingly. At even larger $\epsilon > 0.5$ the pinned pattern is the only possibility because the coarse solutions cease to exist [22].

Summarizing the results for a range of P_{het} at fixed $G=0.1$ and $\bar{h}=2.5$ we obtain the ''morphological phase diagram'' Fig. 4. Coarsening prevails for low values of $\epsilon^* P_{het}/P_c$, while for large values the pattern pins to the heterogeneity as desired [22]. At intermediate values multistability is found where the initial condition selects the final outcome.

(v) *Transversal stability*. The transversal stability of the pinned profiles $(P=P_{het})$ can be obtained from the eigenvalues λ of small perturbations $\delta h(x)\exp(\lambda t)[\exp(iky) + \text{c.c.}]$. We observe a long wavelength instability (reminiscent of the Rayleigh instability) at small ϵ on a length scale much larger than the longitudinal modes. The most dangerous branch of transversal perturbations emerges from the zero eigenvalue representing mass conservation in the film. For $\epsilon = 0.001$ for instance, we found that the fastest growing mode had a wavelength of $\approx 900 = 18 P_{het}$ [see Fig. 1(c)]. The transversal modes are stabilized for parameters above the solid curve in Fig. 4. For the present choice of $\Pi(h)$ and $G, \bar{h}$ the transversal instability restricts the stability range of the pinned solution more than longitudinal coarsening.

(vi) *Summary*. We have studied the conditions for successful templating or pinning of thin films that are unstable to spinodal dewetting. A periodic stripe pattern can be pinned if the heterogeneous substrate suppresses the transverse and longitudinal instabilities typical for a homogeneous substrate. While previous studies have employed direct numerical simulation to study the dynamics of thin films, we have used numerical bifurcation and stability computations. This allows an efficient scanning of parameters characterizing the heterogeneous substrate and the film dynamics. Comparing the two length scales P_c and P_{het} of spinodal dewetting and heterogeneity, respectively, we find that patterns are not pinned to heterogeneities on a much smaller scale than P_c, and that smaller P_c need weaker heterogeneities to pin the pattern. In consequence, templating can be best controlled by choosing the initial mass of fluid which yields the smallest P_c, i.e., the film thickness where the derivative $-\partial_{hh} f(h,x)|_{\bar{h}}$ is maximal (for constant G), see also Ref. [27]. The transition from coarsening to pinning is hysteretic, giving rise to an extended region where the desired pinned pattern coexists with coarser structures. Our results and the methodology also apply to other strategies of stabilizing a periodic pattern including introduction of anisotropy or convective flows [28].

We acknowledge support by the Deutsche Forschungsgemeinschaft (Grant Nos. BA1225/5-1 and TH781).

[1] L. Rockford, Y. Liu, P. Mansky, T.P. Russell, M. Yoon, and S.G.J. Mochrie, Phys. Rev. Lett. **82**, 2602 (1999).
[2] M. Mertig, R. Kirsch, W. Pompe, and H. Engelhardt, Eur. Phys. J. D **9**, 45 (1999).
[3] H. Gau, S. Herminghaus, P. Lenz, and R. Lipowsky, Science **283**, 46 (1999).
[4] D.E. Kataoka and S.M. Troian, Nature (London) **402**, 173 (1999).
[5] M. Gleiche, L.F. Chi, and H. Fuchs, Nature (London) **403**, 794 (2000).
[6] A.M. Higgins and R.A.L. Jones, Nature (London) **404**, 476 (2000).
[7] P. Lenz and R. Lipowsky, Phys. Rev. Lett. **80**, 1920 (1998).
[8] C. Bauer and S. Dietrich, Phys. Rev. E **61**, 1664 (2000).
[9] R. Konnur, K. Kargupta, and A. Sharma, Phys. Rev. Lett. **84**, 931 (2000).
[10] K. Kargupta and A. Sharma, Phys. Rev. Lett. **86**, 4536 (2001).
[11] U. Thiele, M. Mertig, and W. Pompe, Phys. Rev. Lett. **80**, 2869 (1998).
[12] J. Bischof, D. Scherer, S. Herminghaus, and P. Leiderer, Phys. Rev. Lett. **77**, 1536 (1996).
[13] G. Reiter, Phys. Rev. Lett. **68**, 75 (1992).
[14] S. Herminghaus *et al.*, Science **282**, 916 (1998).
[15] A. Sharma and R. Khanna, Phys. Rev. Lett. **81**, 3463 (1998).
[16] U. Thiele, M.G. Velarde, and K. Neuffer, Phys. Rev. Lett. **87**, 016104 (2001).
[17] L.M. Pismen and Y. Pomeau, Phys. Rev. E **62**, 2480 (2000).
[18] M. Bestehorn and K. Neuffer, Phys. Rev. Lett. **87**, 046101 (2001).
[19] U. Thiele, M.G. Velarde, K. Neuffer, and Y. Pomeau, Phys. Rev. E **64**, 031602 (2001).
[20] A. Oron, S.H. Davis, and S.G. Bankoff, Rev. Mod. Phys. **69**, 931 (1997).

[21] J. N. Israelachvili, *Intermolecular and Surface Forces* (Academic Press, London, 1992).

[22] We observed the limiting saddle-node bifurcations of all stable solutions with $P=nP_{het}$ and $2<n\leqslant 10$ at lower values of ϵ and P_{het} than those for $P=2P_{het}$.

[23] E. Doedel, A. Champneys, T. Fairfrieve, Y. Kuznetsov, B. Sandstede, and X. Wang, *AUTO97: Continuation and Bifurcation Software for Ordinary Differential Equations* (Concordia University, Montreal, 1997).

[24] Space was discretized by 64 Fourier modes and the spectrum of eigenvalues and the corresponding eigenmodes are calculated from the linearization of Eq. (1) around the stationary solutions.

[25] L. Brusch, H. Kühne, U. Thiele, and M. Bär (unpublished).

[26] K. Kawasaki and T. Ohta, Physica A **116**, 573 (1982).

[27] K. Kargupta, R. Konnur, and A. Sharma, Langmuir **16**, 10 243 (2000).

[28] A.A. Golovin, A.A. Nepomnyashchy, S.H. Davis, and M.A. Zaks, Phys. Rev. Lett. **86**, 1550 (2001).